Article:

Luhaib, SWO, Bakr, MS orcid.org/0000-0002-2900-8511, Somjit, N orcid.org/0000-0003-1981-2618 et al. (1 more author) (2019) Design and Characterisation of HE11 Dual-Mode Dielectric-Loaded Filter for Cellular Base Station Applications. International Journal of Electronics, 106 (10). pp. 1530-1542. ISSN 0020-7217

https://doi.org/10.1080/00207217.2019.1600739

Design and Characterisation of HE11 Dual-Mode Dielectric-Loaded Filter for Cellular Base Station App

Journal:	*International Journal of Electronics*
Manuscript ID	TETN-2018-1047.R1
Manuscript Type:	International Journal of Electronics (2501-4500 word limit)
Date Submitted by the Author:	24-Feb-2019
Complete List of Authors:	Luhaib, Saad; University of Leeds School of Electronic and Electrical Engineering, Pollard Insitute; College of Engineering, Electrical Engineering Bakr, Mustafa; University of Leeds School of Electronic and Electrical Engineering, Pollard Insitute Somjit , Nutapong; University of Leeds School of Electronic and Electrical Engineering, Pollard Institute Hunter, Ian; University of Leeds School of Electronic and Electrical Engineering, Pollard Institute
Keywords:	Filters, Resonators, Dual-mode dielectric resonator, Bandpass, Base station filters

Note: The following files were submitted by the author for peer review, but cannot be converted to PDF. You must view these files (e.g. movies) online.

IJE_HE11 -final - Copy.rar

ARTICLE TEMPLATE

Design and Characterisation of HE_{11} Dual-Mode Dielectric-Loaded Filter for Cellular Base Station Applications

Saad W. O. Luhaib[a,b], Mustafa S. Bakr[a], Nutapong Somjit[a] and Ian C. Hunter[a]

[a]School of Electronic and Electrical Engineering, University of Leeds, Leeds, UK;
[b]Electrical Engineering Department, University of Mosul, Mosul, Iraq

ARTICLE HISTORY
Compiled February 24, 2019

Abstract
This paper presents a HE_{11} dual-mode dielectric-loaded bandpass filter for cellular base station applications. The filter consists of a ceramic puck that is placed centrally on the base of a metallic housing. The resonator offers a size reduction ratio of approximately 7:1 compared with equivalent air-filled coaxial filters. The filter is designed at a resonant frequency of 2.05 GHz and bandwidth of 50 MHz. The spurious-free window (SFW) was 500 MHz from the fundamental frequency. A fourth order dual-mode bandpass filter is designed, fabricated, and tested to validate the proposed approach. A good agreement between the measurement and simulation results is demonstrated.

KEYWORDS
Dual-mode dielectric resonator, Bandpass filter, Base station filters.

1. Introduction

The miniaturisation of filters is a key requirement to enable the wide deployment of multiple-input multiple-output (MIMO) systems in wireless communications. It also reduces the power dissipation in RF transceivers by placing filters next to antennas and thus making the coaxial cable connecting them redundant. Dielectric resonators are traditionally used to replace bulky TEM and waveguide filters while maintaining good electrical performance (Cohn, 1968; Hunter, 2001; Mansour, 2004). The use of multi-mode degenerate resonances enables further size reduction at the expense of system complexity. Since the proposal of dual-mode dielectric resonators in (Guillon et al., 1980), a vast number of dual-mode dielectric resonator filters have been reported in the literature. Dual-mode dielectric resonators can be divided into three main categories. The first category is based on the operation of HE_{11} or EH_{11} degenerate hybrid-modes. In the second category, TE degenerate modes are utilised to design compact and moderate Q-factor filters (Bakr et al., 2016; Luhaib et al., 2018; Luhaib et al., 2018; Sandhu and Hunter, 2016). The third category uses the TM degenerate modes to design microwave filters (Rezaee and Höft, 2016). The work in this paper concerns the design of compact and easy to manufacture HE_{11} dielectric resonator filters. Dual-mode dielectric resonator (DR) loaded cavity filters were proposed in(Bakr et al., 2017;

Contact Saad W. O. Luhaib. Email: saadw1981@gmail.com

Chi et al., 1997; Fiedziuszko, 1983; Hunter et al., 1999; Li et al., 2009; Memarian and Mansour, 2009) to enable further size and mass reduction, ease of fabrication and the realisation of finite transmission zeros. In (Fiedziuszko, 1983), a ceramic disc was suspended in the middle of a metallic cavity to design HE_{11} dual-mode filters with a high Q-factor and spurious free window ratio of 1.075. A semi-cut dielectric puck was proposed in (Memarian and Mansour, 2009) achieving a spurious-free window ratio of 1.24. However, a 50% volume reduction have been provided by (Fiedziuszko, 1983; Memarian and Mansour, 2009) compared with coaxial TEM filter. In (Chi et al., 1997) a new HE_{11} dual-mode resonator was reported in which a metal rod was inserted in the middle of a hollow DR to design reduced size microwave filters. A conductor loaded dielectric resonator was proposed by Hunter et al. and Bakr et al. (Bakr et al., 2017; Hunter et al., 1999; Li et al., 2009) where a metallic disc was placed on top of a grounded dielectric puck. However, it does degrade the resonator Q-factor.

This paper proposes a dual-mode DR filter offering a significant improvement in size, losses and spurious-free window compared with other literatures on HE_{11} dual-mode DR filters. The DR structure is composed of a dielectric puck that is placed on the base of a metallic cavity. The degenerate HE_{11} dual-mode is the fundamental resonance for this filter. The inter-resonator coupling is achieved by etching a vertical circular hole in the dielectric puck placed at 45^0 with respect to the resonant modes. A coaxial probe was attached to a metal grounded post to achieve the required input/output and inter-cavity couplings. A hardware prototype of four-pole bandpass filter was designed, fabricated and tested to validate the proposed approach.

2. Configuration of the Proposed Resonator

Traditionally, dielectric pucks are suspended in the middle of a metallic housing to design $TE_{01\delta}$ filters. The approach used in this work is to move the dielectric puck towards the base of the cavity thus $TE_{01\delta}$ goes up in frequency and HE_{11} goes down in frequency. When the puck is in contact with the base of the metallic cavity, HE_{11} is the fundamental resonance. Figure 1 shows a schematic diagram of the reported resonator. The dimensions of the metallic cavity are defined as 40 mm height H and diameter D respectively. An eigenmode solver was used to calculate the resonant frequency of the first five modes as a function of cavity to puck height (H/h) as shown in Figure 2. It can be seen that the fundamental mode is HE_{11} for H/h > 1.3. Increasing the

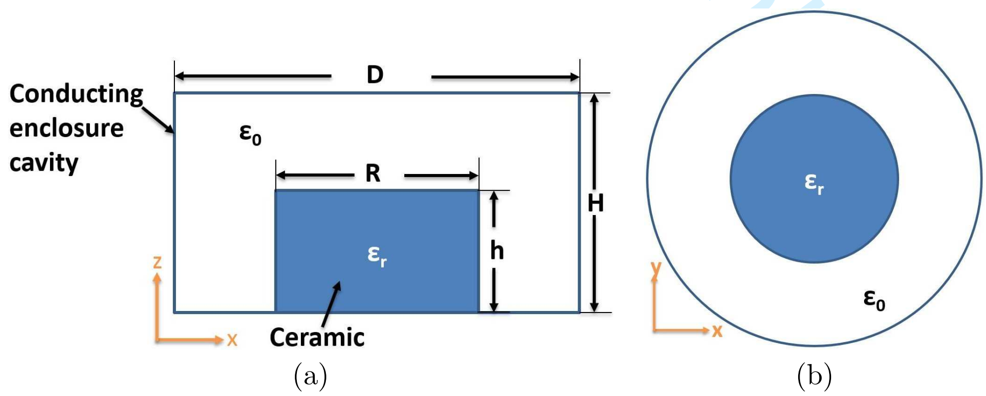

Figure 1. Diagram of dielectric resonator in conducting cavity (a) Front view, (b) Top view.

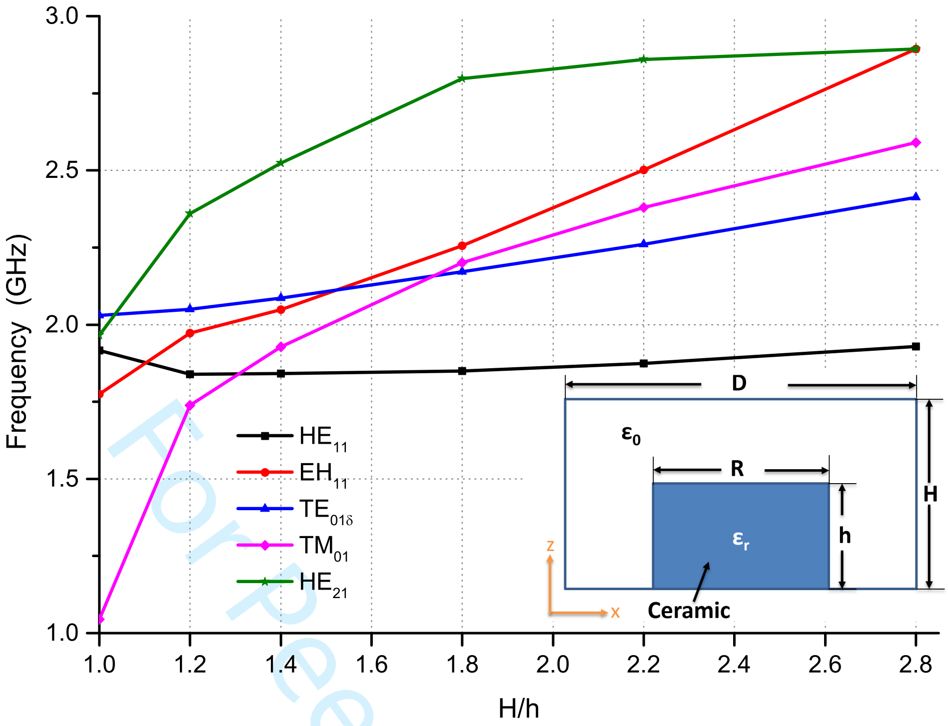

Figure 2. Mode chart for shorted dielectric against H/h.

ratio of H/h leads to better spurious window while not significantly affecting the fundamental resonance. The resonator dimensions were optimised to achieve good spurious performance and high Q-factor in a small size. The optimum dimensions are defined as 34 mm, and 20 mm for metallic housing and dielectric puck diameters respectively. The height of the cavity and dielectric puck are defined as 20 mm and 14 mm respectively. The optimised resonator dimensions offers a size reduction ratio of 7:1 compared to equivalent air-filled coaxial filters. Figure 3 shows the E and H-field patterns of the degenerate HE_{11} modes of the proposed cavity. In the case of suspending a ceramic in the middle of a metallic cavity, the E-field of the HE_{11} is circulating around the axial of the ceramic puck. However, when the puck is placed on the base of the metallic housing, the E-field exhibits a semi-circle axial rotation and thus HE_{11} moves down in frequency. It is also observed that most of the E-field is concentrated in the middle of the ceramic puck while the rest of it is partially perpendicular to the side wall of the metallic housing. Moreover, the magnetic field is almost entirely concentrated in the ceramic puck however, it could be used for input to resonator coupling despite being weak outside the ceramic puck.

To design a filter, we need to determine all types of couplings such as external, inter-resonator and inter-cavity couplings as will be shown in the next subsections.

2.1. Input/Output coupling

As above-mentioned, the E and H-fields can be utilised to provide the required I/O to resonator couplings. A coaxial probe was attached to a metal ground post designed for I/O coupling, as shown in Figure 4. A tuning screw element above the metal post

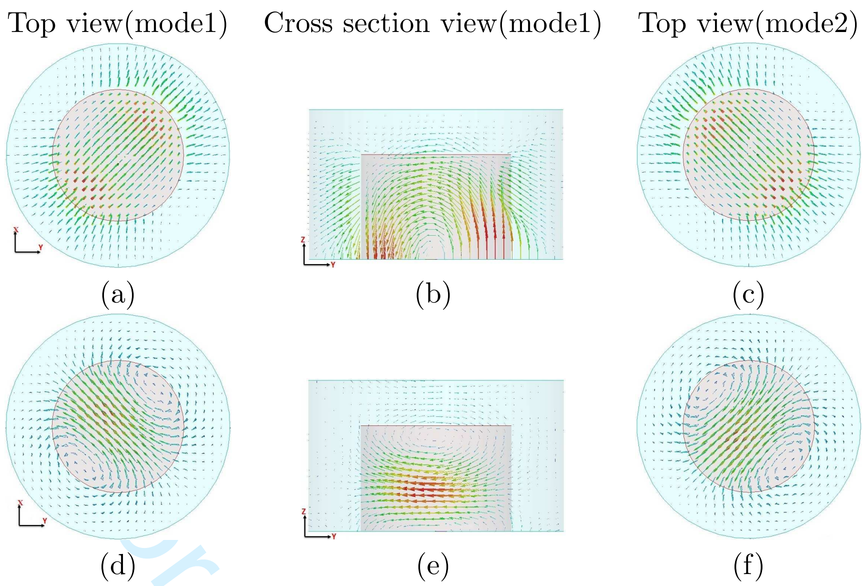

Figure 3. Field distributions of HE_{11} dual-mode resonator (a-c) Electric field, (e-f) Magmatic field

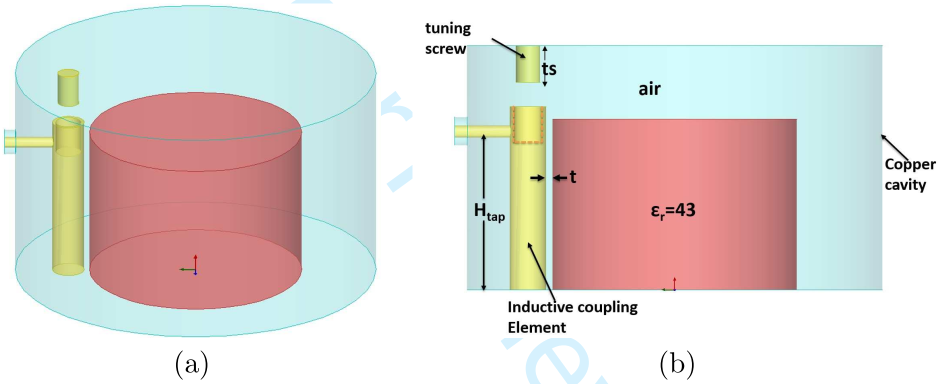

Figure 4. Coupling mechanism for HE_{11} dual-mode (a) 3D view, (b) side view

was used to tune the capacitance of the probe and correct any imperfections in the hardware prototype. In order to have good control of the coupling, a hollow space was provided inside the post. The Q_e is calculated from the group delay response and using the formulas given in 1 (Hong, 2000):

$$Q_e = \frac{\omega_0 \tau_d}{4} \tag{1}$$

Where τ_d is the group delay in second. Figure 5 illustrates the external Q- factor against the distance between the dielectric puck, the inductive post (t) and the length of the tuning screw (ts). Clearly, the relationship between the Q_e and the (t) is directly proportional. The maximum bandwidth is achieved at t=0.3 mm, which is not a wide bandwidth. As shown in the Figure 5(top-X Y-right), when t=0.5 mm the screw can be incorporated to decrease the Q_e coupling that changes from about 60 to 32, when the length of the screw changes by about 2 mm.

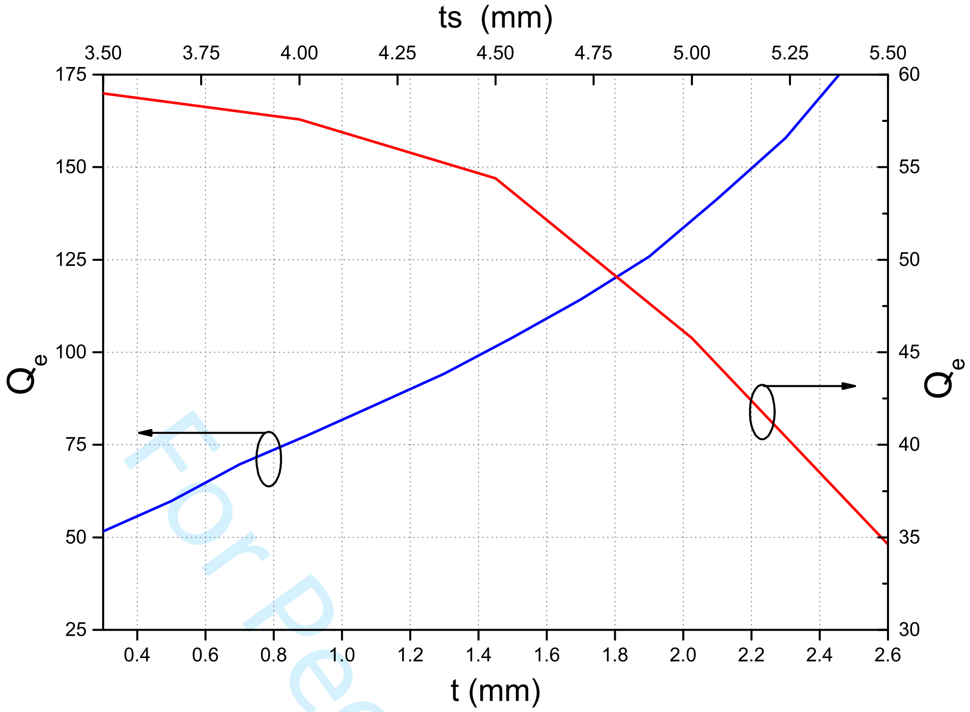

Figure 5. External quality factor (Q_e) against t and ts.

2.2. Inter-resonator coupling

The effective method to implement the inter-resonator coupling is by etching a vertical circular hole in the dielectric puck placed at 45^0 with respect to the two degenerate modes as shown in Figure 6. The coupling can be determined by HFSS simulator by applying the equation below (Hagensen, 2010) :

$$K = f_H - f_L \tag{2}$$

where f_H and f_L are is the frequency of the upper and lower peak respectively. The coupling bandwidth against the distance between the centre of the DR and the hole (X_f) with varying the hole radius (re), which is measured in mm, is presented in Figure 6. Bell-shaped behaviour was observed for the coupling at 7 mm of X_f which gives the maximum coupling for all the recorded values for re. A good diversity of bandwidth can be achieved by this technique which ranges up to 90 MHz at 2.6 mm.

3. Design of HE_{11} Dual-Mode Bandpass Filter

A 4^{th} order Chebyshev dual-mode filter was designed with a centre frequency of 2.05 GHz, bandwidth of 50 MHz and return loss (L_R) of 20 dB at the passband. The coupling matrix and Chebyshev topology with FBW=2.439% are shown below. The I/O external quality factors and the coupling coefficients are computed by coupling matrix synthesis (CMS) software. The Q_e can be found by using equation 3 (Ness, 1998) and the coupling can be determined by multiplying the normalised coupling in

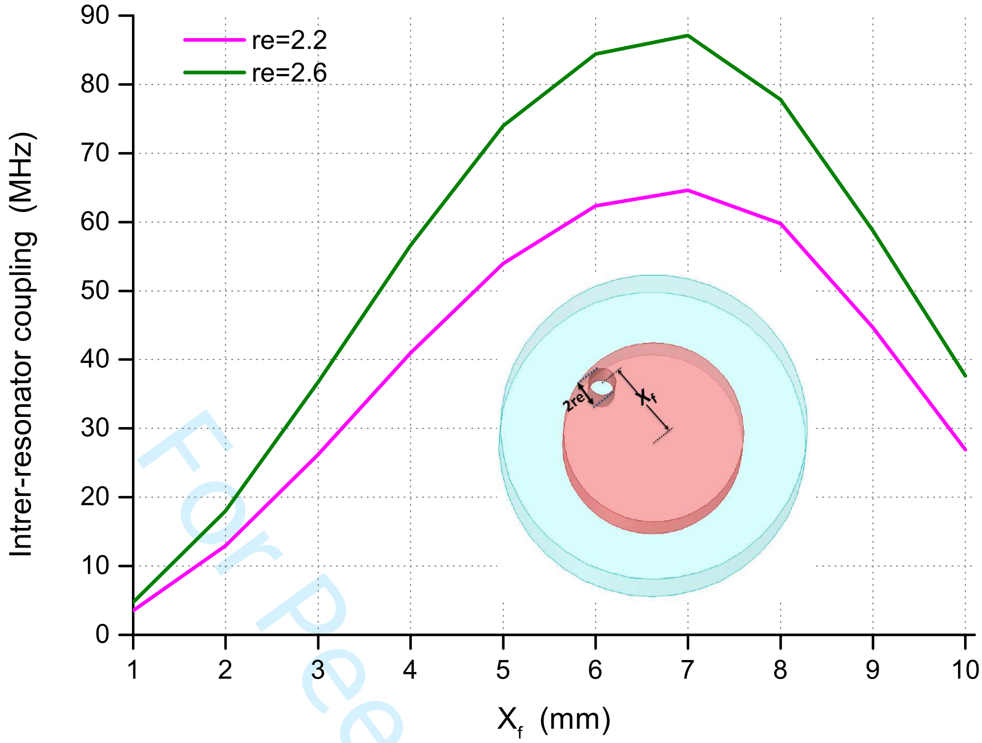

Figure 6. Inter resonator coupling bandwidth varying with radius (re) and (X_f).

CM by the bandwidth.

$$Q_e = \frac{f_0}{BW * M_{S1}^2} \tag{3}$$

where M_{S1} is the I/O normalized coupling from coupling matrix.

$$M = \begin{array}{cc} & \begin{array}{cccccc} S & 1 & 2 & 3 & 4 & L \end{array} \\ \begin{array}{c} S \\ 1 \\ 2 \\ 3 \\ 4 \\ L \end{array} & \begin{bmatrix} 0 & 1.035 & 0 & 0 & 0 & 0 \\ 1.035 & 0 & 0.91 & 0 & 0 & 0 \\ 0 & 0.91 & 0 & 0.7 & 0 & 0 \\ 0 & 0 & 0.7 & 0 & 0.91 & 0 \\ 0 & 0 & 0 & 0.91 & 0 & 1.035 \\ 0 & 0 & 0 & 0 & 1.035 & 0 \end{bmatrix} \end{array}$$

Figure 7 presents the configuration of the 4^{th} order filter in HFSS which consists of two copper cavities and two ceramic pieces which were short-circuited from the backside. All intra-cavity couplings were implemented by an inductive grounded post with a tuning screw on each post to control the coupling bandwidth. To realize the filter, all coupling coefficients from the coupling matrix(CM) need to be converted to physical dimensions by using the coupling equivalence values in Figure 7, as provided in Table 1.

Figure 8 shows the broadband response of the 4^{th}-order Chebyshev filter at $\theta_1 = 315^0$ and $\theta_2 = 225^0$. It can be observed that the bandwidth of the filter at -16 dB was

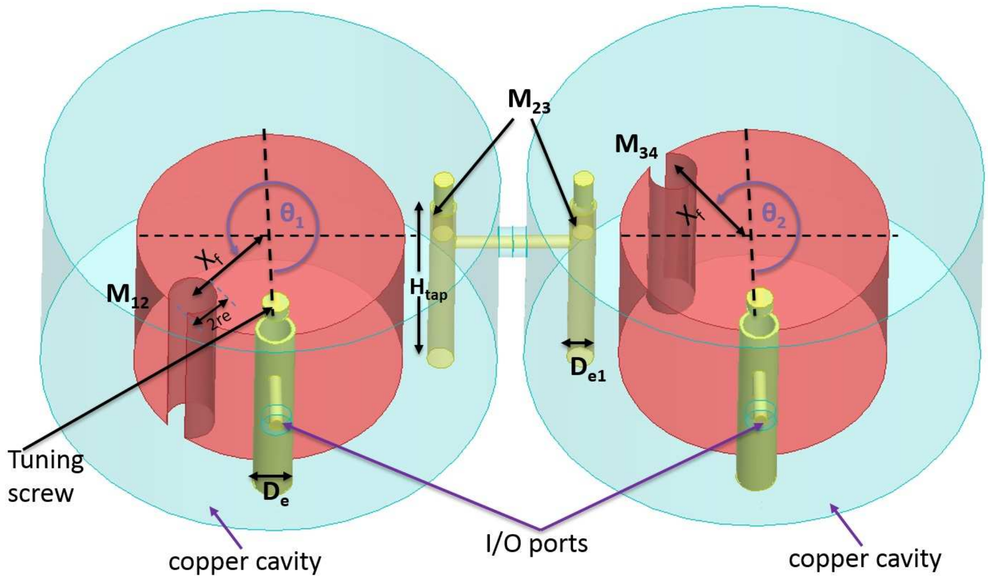

Figure 7. Configuration of HE_{11} dual-mode 4^{th} order filter in HFSS.

Table 1. Typical dimensions of 4^{th} order filter HE_{11} dual-mode.

Coefficient No.	Distance from the centre (mm)	Diameter of elements (mm)	H_{tap} (mm)	Height of etching hole (mm)
M_{S1}=M_{4L}	12	3	13	-
M_{23}	12.8	2	10	-
$M_{12} = M_{34}$	9	4.4	-	14

50 MHz and therefore it meets the requirements of cellular systems. The insertion loss at the resonant frequency 2.065 GHz is less than 0.3 dB and the extracted unloaded Q-factor is slightly more than 4800, while the losses in Q are about 500 compared with eigen-mode analysis. Furthermore, the lower spurious mode is about 2.55 GHz, which means the spurious-free window is about 500 MHz instead of 444 MHz as shown in eigen-mode analysis; also, the maximum isolation was 60 dB and 75 dB for the upper and lower band respectively.

4. Implementation of the HE_{11} dual-mode filter

Figure 9 shows a photograph of the fabrication of a 4^{th} order HE_{11} dual-mode filter. The rectangular filter has dimensions of 80×44×30 mm while the other cavity dimensions and the properties of the material were the same as those mentioned in section 3. Six tuning screws of 3 mm in diameter were positioned on the top lid of the cavity to fine-tune the coupling coefficients and all probes were fabricated of copper. A Teflon probe with 2 mm diameter provided a good contact between the ceramic and the base of the copper cavity. S-parameter measurement is achieved by using an Agilent E5071C Network Analzser. Two-port calibration was performed by using an Agilent N4431-60006 Electronic Calibration Module prior to the measurement. Figure 10 shows the S-parameters found experimentally and modelled for a 4^{th} order Chebyshev filter around the in-band response at $\theta_1 = 225^0$ and $\theta_2 = 135^0$. It can be

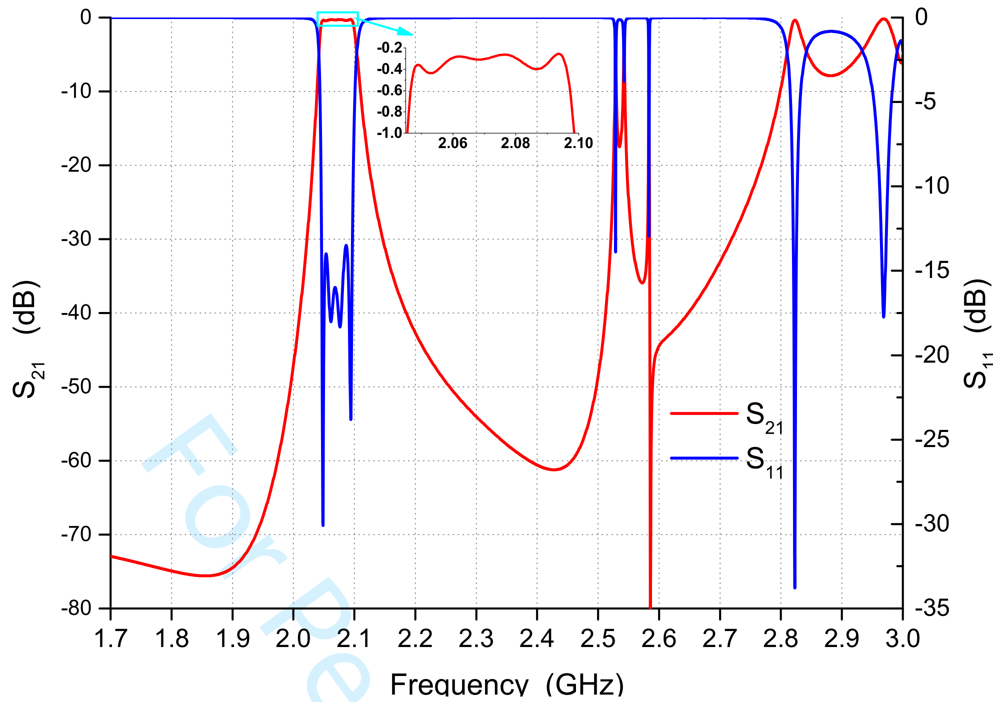

Figure 8. Broadband simulated response of 4^{th} order HE_{11} dual-mode filter.

observed that the measured bandwidth of the filter at -10 dB was equal to 56 MHz, which increased to about 6 MHz compared with the simulation results. This is due to the slight misalignment of the dielectric puck when placed on the bottom of the metallic housing. The insertion loss at the resonant frequency 2.069 GHz is approximately 0.71 dB and the extracted unloaded Q-factor from the group delay is slightly more than 3800 where the Q_u is equal to the simulation result. Figure 11 shows the measured and simulated broadband response of a 4^{th} order Chebyshev filter. It can be seen that the lower spurious mode is about 2.55 GHz, which means the spurious-free window is about 500 MHz instead of 444 MHz as shown in the eigen-mode analysis. Also, the maximum isolation was 80 dB for both the upper and lower bands. There is a good agreement between the measurement and simulation results. Figure 12 presents the performance of the practical filter with varying two tuning screws (H_T)that have a diameter of 3 mm. It can be seen that the TZs in the lower band shifted up by 61 MHz. The TZs around the $TE_{01\delta}$ were converted from the imaginary axis to a complex axis along the H_T, which changed from 0 to 18 mm. Figure 13 presents the simulated and measured response of the 4^{th} order HE_{11} dual-mode filter at $\theta_1 = 315^0$ and $\theta_2 = 135^0$. From the figure, it can be seen that the measurement result has a good agreement with the simulation result. The IL in the resonance frequency was similar in both cases while the measured Bw was increased by 6 MHz. The performance of the broadband response in Figure 14 is similar to the simulation, which has a pair of imaginary TZs in each side of the resonance frequency. The TZs occurred at 2.21 GHz and 1.928 GHz.

Table 2 illustrates the figure-of-merits and extensive comparisons between the novel HE_{11} dual-mode resonator designs and the published research works with the same dual-mode.

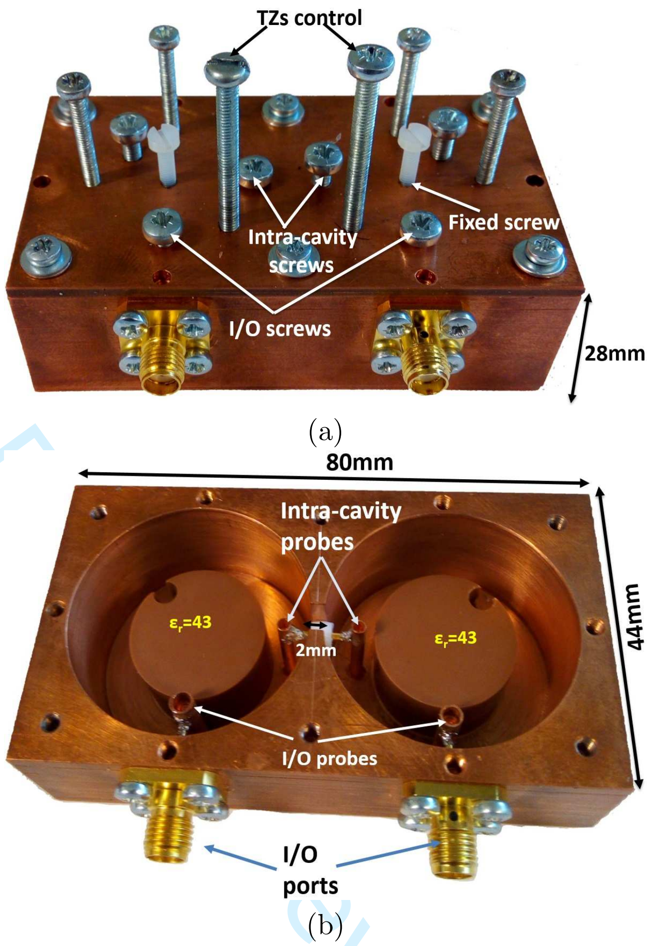

Figure 9. Fabricated 4^{th} degree HE_{11} dual-mode bandpass filter (a) close with top lid, (b) open without top lid.

5. Conclusion

A HE_{11} dual-mode 4^{th} order filter with high Q-factor has been designed, fabricated and tested. The ceramic was shorted from the bottom side to the base of the copper cavity. The filter offers a significant reduction in volume compared with equivalent air-filled coaxial filter. The I/O and the intra-cavity couplings were implemented by connecting the coaxial probe to the grounded post. The simulation and measured results shows good agreement. The position of the inter-resonator hole had a significant effect on the position of TZs as proven by the simulation and measured results. A TZ was observed no matter where the hole was oriented. The number of TZs above the inband is equal to that of the lower band. A good agreement between the measurement and simulation results has been demonstrated.

References

Bakr, M. S., Luhaib, S. W. O., and Hunter, I. C. (2016). A novel dielectric-loaded dual-mode cavity for cellular base station applications. In *2016 46th European Microwave Conference (EuMC)*, pages 763–766.

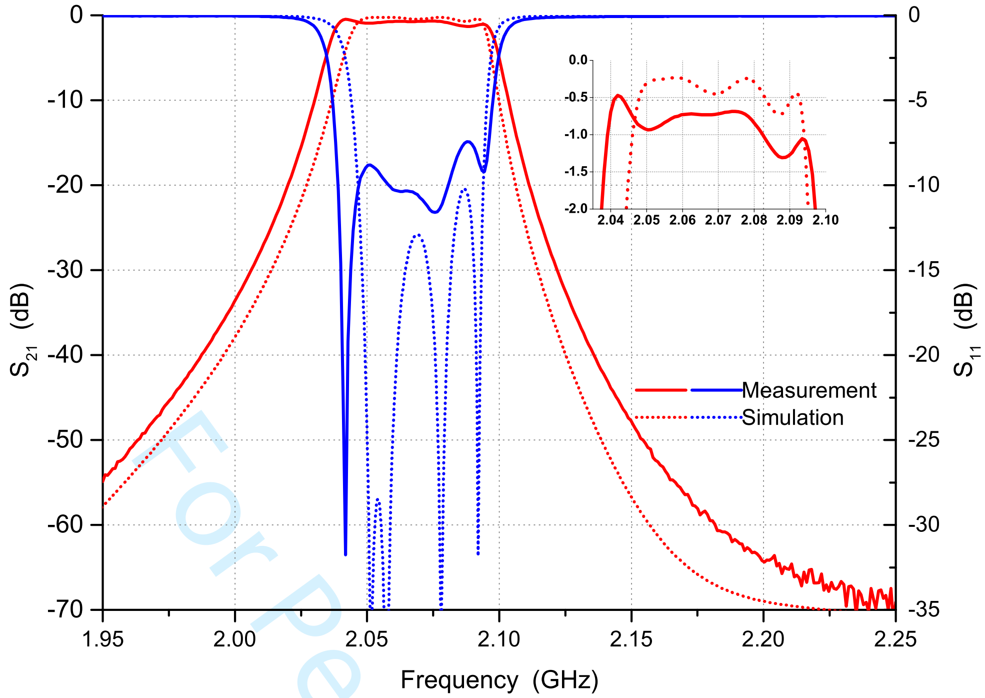

Figure 10. Simulated and measured response of 4^{th} order HE_{11} dual-mode filter at $\theta_1 = 225^0$ and $\theta_2 = 135^0$.

Table 2. Comparison of HE_{11} dual-mode filter with the state-of-the arts.

Ref.	f_r (GHz)	Volume of cavity (cm^3)	Q_u	SFW (MHz)	ϵ_r
(Fiedziuszko, 1983)	3.949	24.29	8000	300	37.25
(Chi et al., 1997)	1.857	250.4	6000	820	metal
(Hunter et al., 1999)	0.942	274.6	6300	480	45
(Memarian and Mansour, 2009)	2.5	55.125	8500	600	38
This work	2.05	18.15	5500	500	43

Bakr, M. S., Luhaib, S. W. O., Hunter, I. C., and Bosch, W. (2017). Dual-mode dual-band conductor-loaded dielectric resonator filters. In *2017 47th European Microwave Conference (EuMC)*, pages 908–910.

Chi, W., Zaki, K. A., Atia, A. E., and Dolan, T. G. (1997). Conductor loaded resonator filters with wide spurious-free stopbands. *Microwave Theory and Techniques, IEEE Transactions on*, 45(12):2387–2392.

Cohn, S. B. (1968). Microwave bandpass filters containing high-q dielectric resonators. *IEEE Transactions on Microwave Theory and Techniques*, 16(4):218–227.

Fiedziuszko, S. J. (1983). Corrections to "dual mode dielectric resonator loaded cavity filters". *IEEE Transactions on Microwave Theory and Techniques*, 31(3):315–315.

Guillon, P., Garault, Y., and Farenc, J. (1980). Dielectric resonator dual modes filter. *Electronics Letters*, 16(17):646–647.

Hagensen, M. (2010). Narrowband microwave bandpass filter design by coupling matrix synthesis (vol 53, pg 218, 2010). *MICROWAVE JOURNAL*, 53(6):130–130.

Hong, J. S. (2000). Couplings of asynchronously tuned coupled microwave resonators. *IEE Proceedings - Microwaves, Antennas and Propagation*, 147(5):354–358.

Hunter, I. (2001). *Theory and Design of Microwave Filters.* Electromagnetics and Radar Series. Institution of Engineering and Technology.

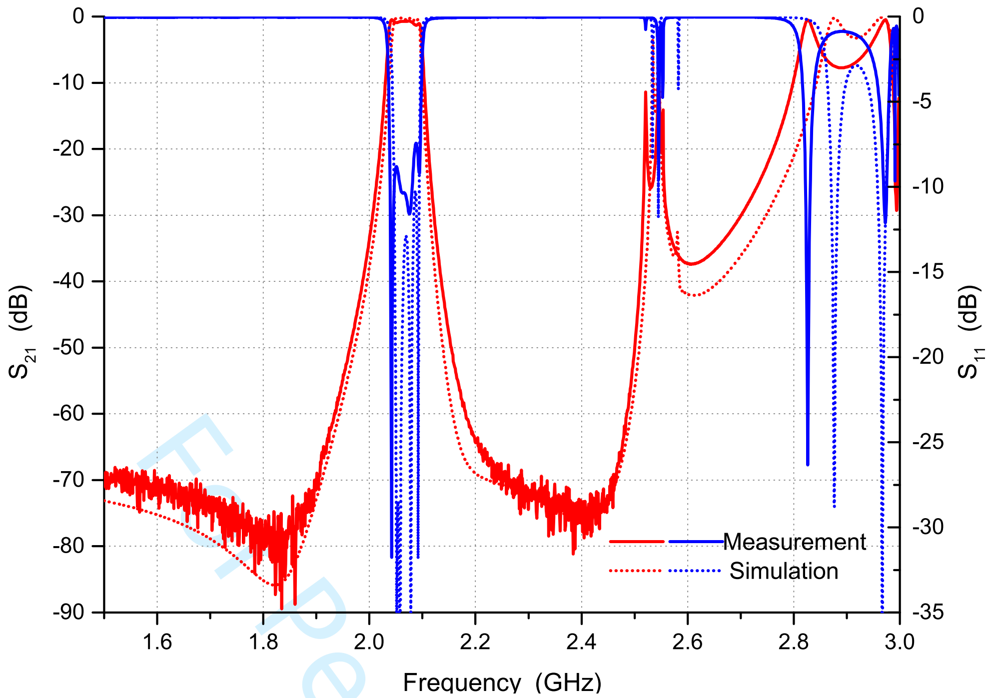

Figure 11. Broadband simulated and measured response for 4^{th} order HE_{11} dual-mode filter at $\theta_1 = 225^0$ and $\theta_2 = 135^0$.

Hunter, I. C., Rhodes, J., and Dassonville, V. (1999). Dual-mode filters with conductor-loaded dielectric resonators. *Microwave Theory and Techniques, IEEE Transactions on*, 47(12):2304–2311.

Li, L., Li, Z.-F., and fu Wei, Q. (2009). Dual-mode filter design based on uniform or stepped impedance resonator. *International Journal of Electronics*, 96(4):373–385.

Luhaib, S., Somjit, N., and Hunter, I. C. (2018). Improvement of the stopband spurious window for a dual-mode dielectric resonator filter by new coupling technique. *International Journal of Electronics*, 105(11):1805–1815.

Luhaib, S. W. O., Somjit, N., and Hunter, I. C. (2018). Spurious stopband improvement of dual-mode dielectric resonator filters using t-shaped coupling probe. *IET Microwaves, Antennas Propagation*, 12(15):2345–2349.

Mansour, R. R. (2004). Filter technologies for wireless base stations. *IEEE Microwave Magazine*, 5(1):68–74.

Memarian, M. and Mansour, R. R. (2009). Dual-mode half-cut dielectric resonator filters. In *Microwave Symposium Digest. MTT '09. IEEE MTT-S International*, pages 1465–1468.

Ness, J. B. (1998). A unified approach to the design, measurement, and tuning of coupled-resonator filters. *IEEE Transactions on Microwave Theory and Techniques*, 46(4):343–351.

Rezaee, P. and Höft, M. (2016). A new class of compact dual-mode dielectric resonator filters. In *2016 IEEE MTT-S International Microwave Symposium (IMS)*, pages 1–3.

Sandhu, M. Y. and Hunter, I. C. (2016). Miniaturized dielectric waveguide filters. *International Journal of Electronics*, 103(10):1776–1787.

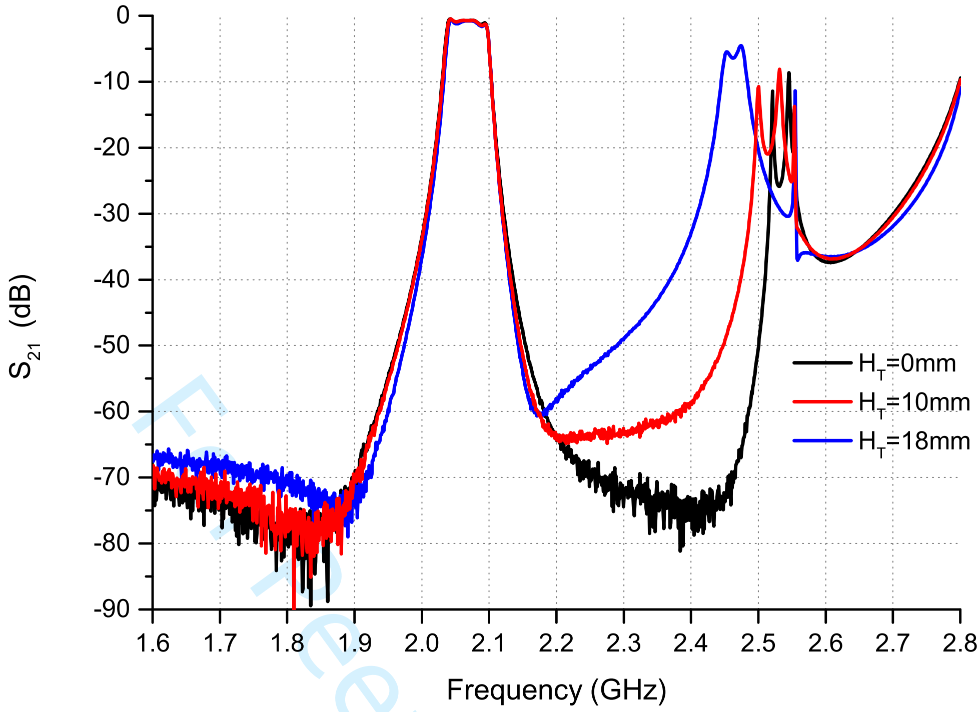

Figure 12. Control the TZ position by two tuning screws in measurement at $\theta_1 = 225^0$ and $\theta_2 = 135^0$.

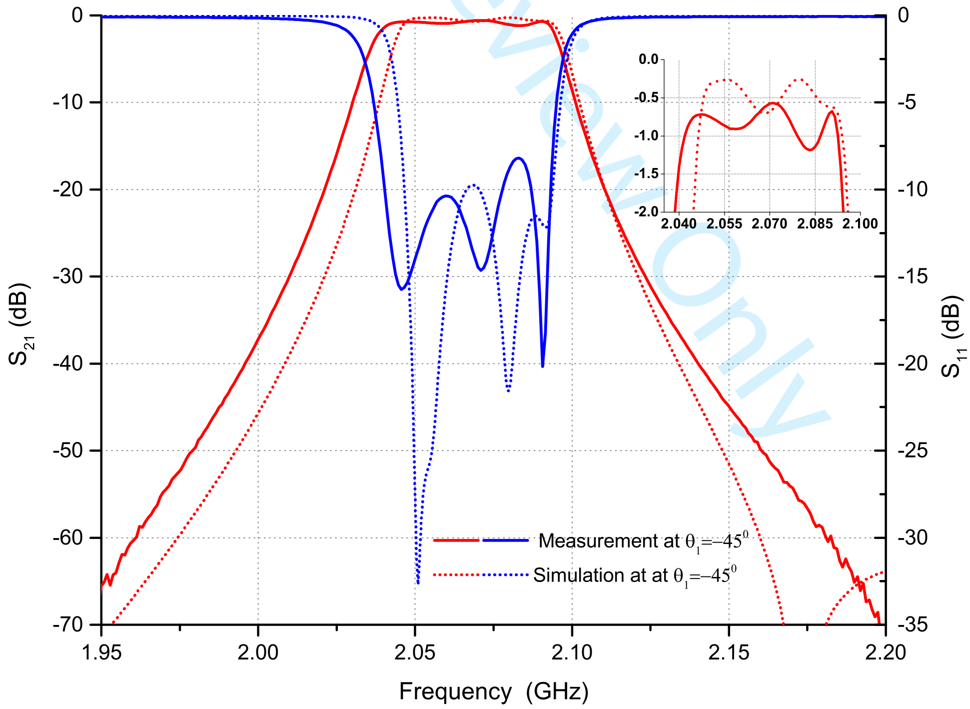

Figure 13. Simulated and measured response of 4^{th} order HE_{11} dual-mode filter at $\theta_1 = 315^0$ and $\theta_2 = 135^0$.

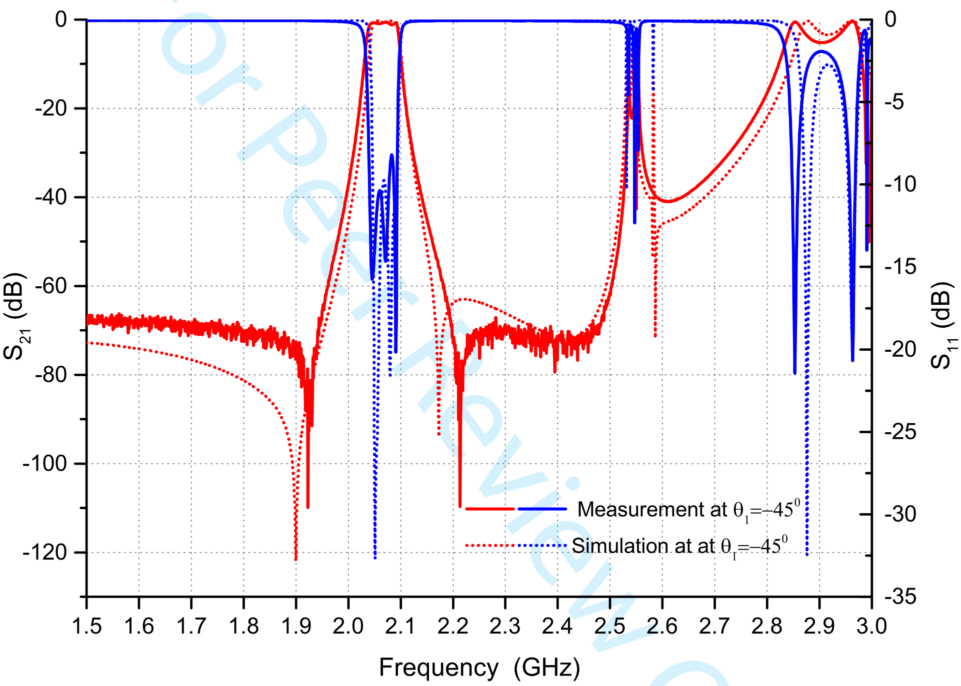

Figure 14. Simulated and measured broadband response of 4^{th} order HE_{11} dual-mode filter at $\theta_1 = 315^0$ and $\theta_2 = 135^0$.